AMSE Journal on Advances in Modeling and Analysis, C, Vol 60, No 5, pp.43-55, 2005

Design of a Robust Fixed-parameter SVC Damping Controller through Graphical Loop-shaping Technique

S. A. Al-Baiyat A. H. M. A. Rahim
Department of Electrical Engineering
K. F. University of Petroleum and Minerals
Dhahran, Saudi Arabia.

Abstract

A novel robust damping controller for a static var compensator (SVC) has been designed using a simple graphical technique. In the robust design, the variations in operations from a nominal condition are modeled as multiplicative unstructured uncertainty. A loop-shaping technique is employed to solve the robust stability and performance constraints in H-∞ space graphically. The robust constant parameter controller designed has been tested for a range of operating conditions considering a number of disturbances on the system. It is observed that the robust controller provides extremely good damping for a good range of operation. The electrical transients as reflected in the system voltage variations are also extremely good.

Keywords

SVC, Power system damping control, robust control, loop-shaping technique.

1. Introduction

Thyristor controlled reactors and capacitors, termed as static var compensators (SVC) are well known to improve power system properties such as steady state stability limits, voltage regulation and var compensation, dynamic over-voltage and under-voltage control, counteracting sub-synchronous resonance, and damp power oscillations [1-3]. The static var compensators are the first generation of flexible ac transmission systems (FACTS) devices. Voltage controlled SVC, as such, does not provide any damping to the power system [4, 5]. However, supplemental signals to the voltage set point can be used to improve system damping [3, 6].

Control design for the nonlinear power system is often carried out through linearized system models. These include EL (exact linearization), LQR (linear quadratic regulator) theory, DFL (direct feedback linearization). DFL was employed by Tso and Wang [7, 8] to generate SVC and other FACTS controllers. The method presents a complex nonlinear control law derived through the solution of Matrix-Riccati equation. More complex methods of disturbances auto-rejection control (DARC) and variable structure adaptive fuzzy sliding mode control were presented by Zhang and Ghazi [9, 10]. Optimum feedback control of SVC for stabilization of a power system was presented in [11]. Most of these linearization based designs are normally handicapped because of their applicability to stability in the small.

One of the important goals of the control engineers is to design 'robust' fixed parameter controllers which will be effective over a large range of operation. Farasangi [12] proposed a robust controller for SVC using H_∞ techniques. H_∞ technique based robust controller was also proposed by Zhao [13]. The designs are often complicated restricting the realization of the controllers.

This article presents a simple and a relatively new technique for robust design of an SVC damping controller. The variations of the operating conditions of the nonlinear power system dynamic relationships have been modeled as multiplicative unstructured uncertainty. A loop-shaping technique [14] has been employed to design the controllers satisfying the robust stability and performance criteria. Simulation results demonstrate that the controller designed damps the electromechanical oscillations for a wide range of operating conditions very effectively. Initial results of this study were reported in [15].

2. Dynamic Model with SVC

A synchronous generator connected to a large power system over a long transmission line, as shown in Fig. 1, is considered for this study. The SVC is placed at the middle of the transmission line which is generally considered to be the ideal site. The generator is assumed to be equipped with an IEEE type-ST excitation system and has a local load connected at its terminal. The synchronous –generator exciter system is modeled in terms of the following 4th order state model. The state variables are the generator rotor angle (δ), speed (ω), the internal voltage (e_q'), and the field voltage (E_{fd}).

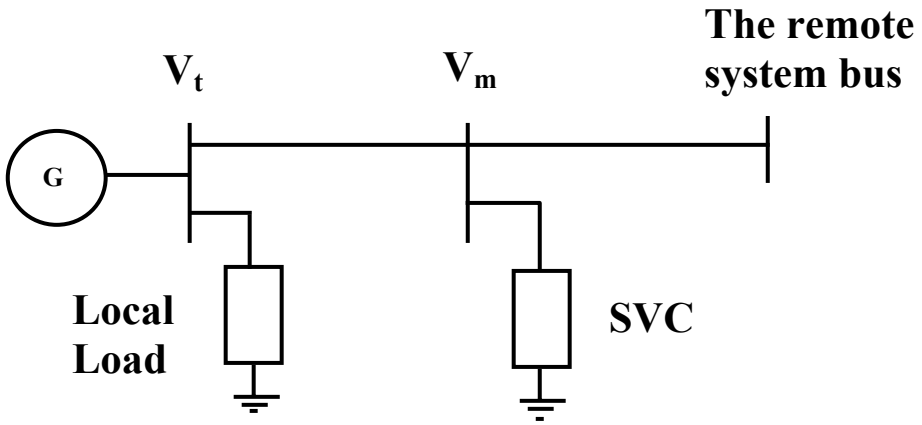

Fig. 1 Power system configuration

$$\dot{\delta} = \omega_o \Delta\omega$$
$$\dot{\omega} = \frac{1}{2H}[P_m - D\Delta\omega - P_e]$$
$$\dot{e}_q^{'} = \frac{1}{T_{do}^{'}}[E_{fd} - e_{qo}^{'} - (x_d - x_d^{'})i_d] \quad (1)$$
$$\Delta\dot{E}_{fd} = \frac{K_r}{T_r}[-\Delta V_t + u_E] - \frac{1}{T_r}\Delta E_{fd}$$

The generator power output (P_e) , terminal voltage (V_t) are expressed in terms of d-q axes generator currents (i_d, i_q) and system reactances [11]. The static var compensator circuit, shown in Fig.2, contains the voltage measuring circuit and the voltage regulator circuit, the output of which is used to control the thyristor firing angle. Normally, the susceptance of the SVC (B) is varied to maintain the mid-bus voltage V_m within its pre-specified tolerance. The supplementary stabilizing signal is added to the output of the voltage regulator for damping control. The variation of the susceptance (B) can be related through the differential equation,

$$\Delta\dot{B} = [-\Delta B + B_o + K_s u_B] / T_s \quad (2)$$

K_s and T_s are the gain and time constants, respectively of the SVC firing angle control circuits. u_B is the input to the thyristor firing angle controller. Combining (2) with the fourth order generator model, the dynamic equations of the generator-SVC system are expressed as,

$$\dot{x} = f[x, u] \quad (3)$$

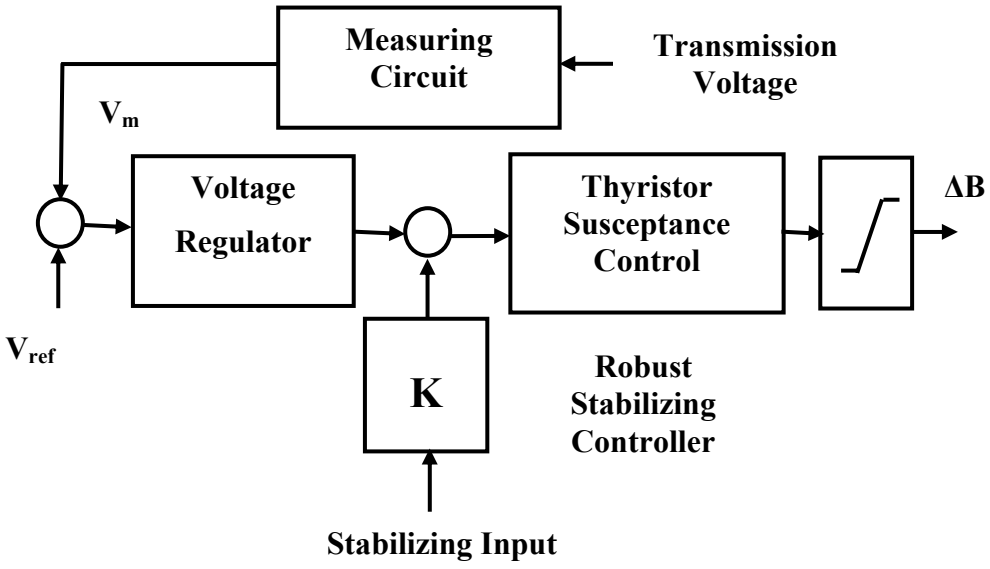

Fig.2 SVC controller block diagram

Linearizing the nonlinear equations around a nominal operating condition, the input-state-output equations are written as,

$$\Delta\dot{x} = A\,\Delta x + Bu \quad (4)$$
$$y = H\,\Delta x \quad (5)$$

Control u is the input to the firing angle (u_B) control circuit. The output y can be appropriately chosen for the control design problem.

3. Robust Control Design

The robust damping control problem can be stated as to find u in (3) which will provide satisfactory damping characteristics to the power system transients. Since controller design with these specifications for the nonlinear system is extremely difficult, if not impossible, the design is carried out by defining a bounded set of transfer function matrices, $\mathcal{G}$, which contains the nominal transfer function $G(s)= H[sI-A]^{-1}B$. The changes in operating conditions of a power system which can be viewed as changes in the coefficient matrix A in (4) are considered as model uncertainties in $\mathcal{G}$ [13,15].In this article these perturbations are modeled as multiplicative uncertainties and robust design procedure is applied to the perturbed linear systems. In the following, a brief theory of the uncertainty model, the robust stability criterion, a graphical design technique termed loop shaping, which is employed to design the robust controller are summarized. Finally, the algorithm for the control design is presented.

3.1 The uncertainty model and robustness criteria

The perturbations from a nominal plant function G is modeled through unstructured uncertainty. For multiplicative representation of unstructured uncertainty, the set $\mathcal{G}$ is defined to contain the perturbed transfer function resulting from the variations in operating conditions, such that [14,16],

$$\mathcal{G}=\{\widetilde{G} \mid \widetilde{G} = (I + \Omega W_2)G\} \qquad (6)$$

Here, W_2 is a fixed stable transfer function, also called the weight, and Ω is a variable transfer function satisfying $\|\Omega\|_\infty <$ 1. The infinity norm (∞-norm) of a function is the least upper bound of its absolute value, also written as $\|\Omega\|_\infty = \sup_\omega |\Omega(j\omega)|$, is the largest value of gain on a Bode magnitude plot. $|W_2(j\omega)|$ provides the uncertainty profile, and in the frequency plane is the upper boundary of all the normalized plant transfer functions away from 1. The actual feedback loop (a) and the reduced closed loop system (b) are shown in Fig. 3. K is the controller transfer function.

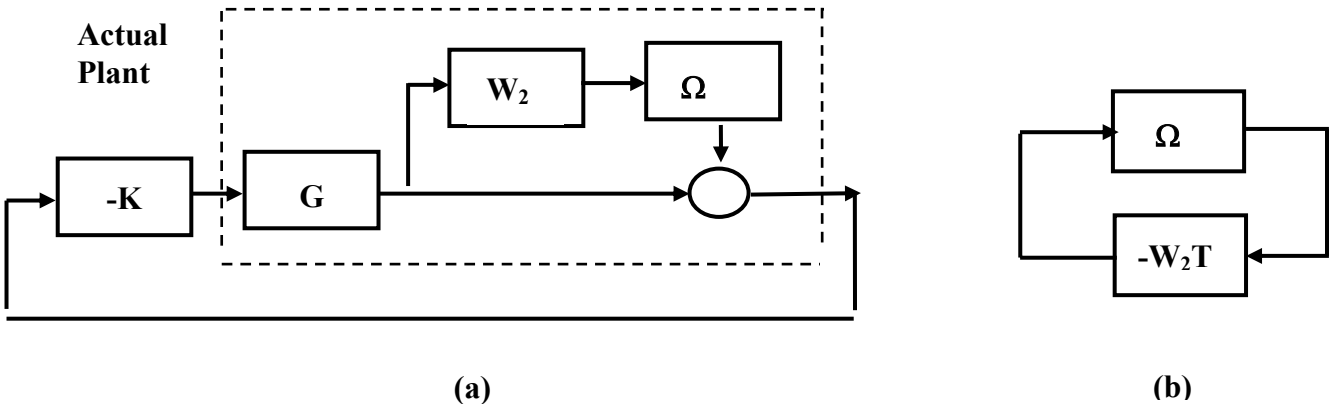

Fig.3 Stability robustness for multiplicative uncertainty at plant output

Consider a multi-input feedback control system given in Fig 4. The controller K provides stability if it provides internal stability for every plant in the uncertainty set $\mathcal{G}$. If L denotes the open-loop transfer function (L=GK), then the sensitivity function S is written as,

$$S = \frac{1}{1+L} \tag{7}$$

The complimentary sensitivity function or the input-output transfer function is,

$$T = 1 - S = \frac{GK}{1+GK} \tag{8}$$

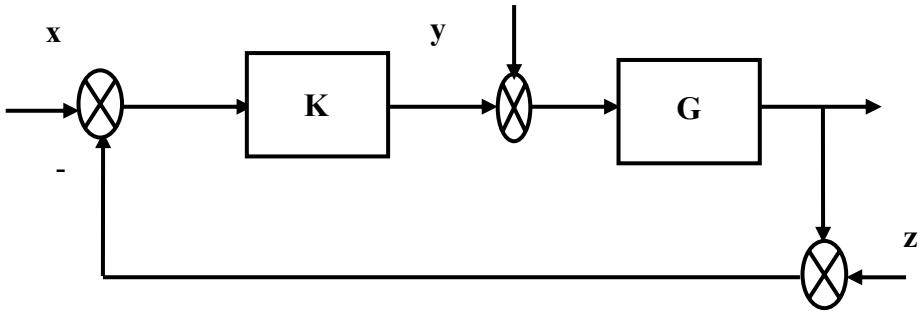

Fig.4 Unity feedback plant with controller.

For a multiplicative perturbation model, robust stability condition is met if and only if $\|W_2 T\|_\infty < 1$. This implies that,

$$\left|\frac{W_2(j\omega)L(j\omega)}{1+L(j\omega)}\right| < 1, \text{ for all } \omega \tag{9}$$

or, $\left|\Omega(j\omega)W_2(j\omega)L(j\omega)\right| < \left|1+L(j\omega)\right|$, for all ω, and $\|\Omega\|_\infty < 1$. (10)

The nominal performance condition for an internally stable system is given as $\|W_1 S\|_\infty < 1$, where W_1 is a real-rational, stable, minimum phase transfer function, also called a weighting function. It can be shown that a necessary and a sufficient condition for robust performance is [14],

$$\left\|\left|W_1 S\right| + \left|W_2 T\right|\right\|_\infty < 1 \tag{11}$$

3.2 The Loop Shaping Technique

Loop-shaping is a graphical procedure to design a proper controller K satisfying robust stability and performance criteria given above. The basic idea of the method is to construct the loop transfer function L to satisfy the robust performance criterion approximately, and then to obtain the controller from the relationship K=L/G. Internal stability of the plants and properness of K constitute the constraints of the method. Condition on L is such that PK should not have any pole zero cancellation.

A necessary condition for robustness is that either or both $|W_1|, |W_2|$ must be less than 1. If we select a monotonically decreasing W_1 satisfying the other constraints on it, it can be shown that at low frequency the open-loop transfer function L should satisfy,

$$|L| > \frac{|W_1|}{1-|W_2|} \tag{12}$$

while, for high frequency

$$|L| < \frac{1-|W_1|}{|W_2|} \approx \frac{1}{|W_2|} \tag{13}$$

At high frequency $|L|$ should roll-off at least as quickly as $|G|$ does. This ensures properness of K. The general features of open loop transfer function is that the gain at low frequency should be large enough, and $|L|$ should not drop-off too quickly near the crossover frequency resulting into internal instability.

The algorithm to generate a control transfer function K can be summarized through the following steps.

1. Obtain the db-magnitude plot for the nominal as well as perturbed plant transfer functions.
2. Construct W_2 satisfying constraint (6).
3. Select W_1 as a monotonically decreasing, real, rational and stable function.
4. Choose L such that it satisfies conditions (12) and (13). The transition at crossover frequency should not be at slope steeper than –20db/decade.
5. Check for the nominal and robust performance criteria given in section 3.1.
6. Test for internal stability by direct simulation of the closed loop transfer function for pre-selected disturbance or input.
7. Repeat steps 4 through 6 until satisfactory L and K are obtained.

4. Simulation Results

For nominal generator power output of 0.8pu at 0.85 lagging power factor the plant transfer function G, considering the generator speed variation as the plant output, is obtained as,

$$G = \frac{0.0339s\ \ (s+32.7)(s+0.74)}{(s+0.548)(s+20)(s+33.03)(s^2+0.1282s+35.97)} \tag{14}$$

Off-nominal power output between the range of 0.3-1.3 pu and power factor of up to 0.8 lag/lead which gave steady state stable situations were considered in the robust design. The log-magnitude vs. frequency plots for the nominal and perturbed plants are shown in Fig.5. Data for the generator-SVC system has been taken from [11].

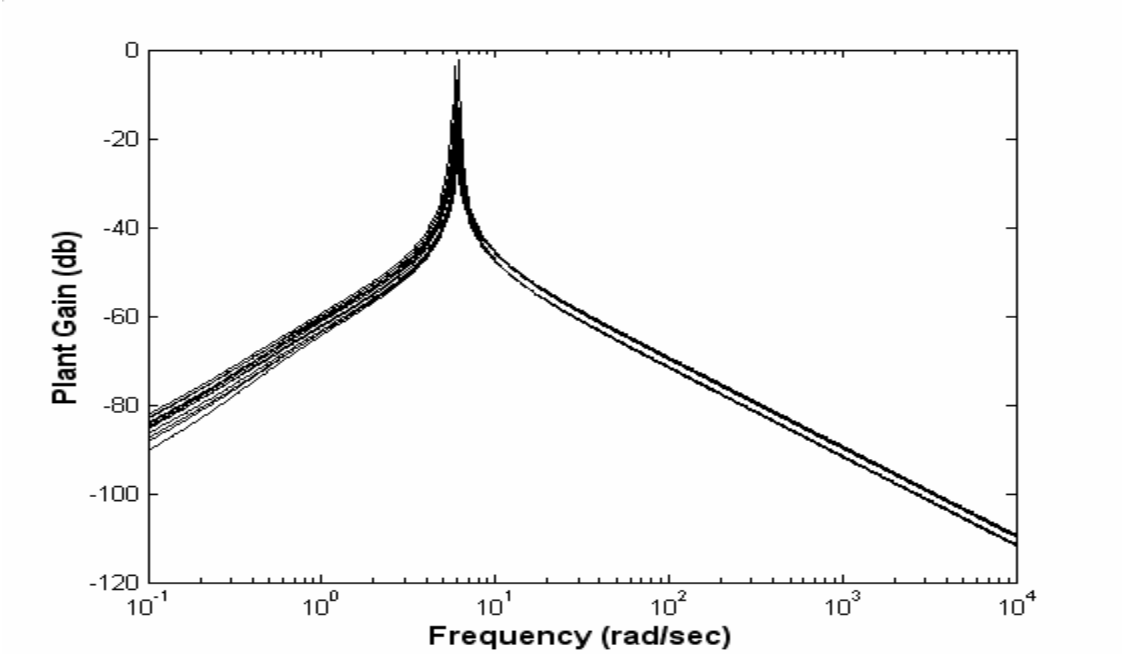

Fig. 5 Bode magnitude diagram of nominal and perturbed plant functions

The quantity $\left|\widetilde{G}(j\omega)/G_{nom}(j\omega)-1\right|$ is constructed for each perturbed plant $\widetilde{G}(j\omega)$ and the upper envelope in the frequency plane is fitted to the function,

$$W_2(s)=\frac{0.2428s^3+3.8506s^2+14.1633s+10.5625}{s^3+1.8s^2+42.9s+21.125} \tag{15}$$

Fig.6 shows the supremum of the functions $\left|\widetilde{G}(j\omega)/G_{nom}(j\omega)-1\right|$ and the fitted upper envelope W_2.

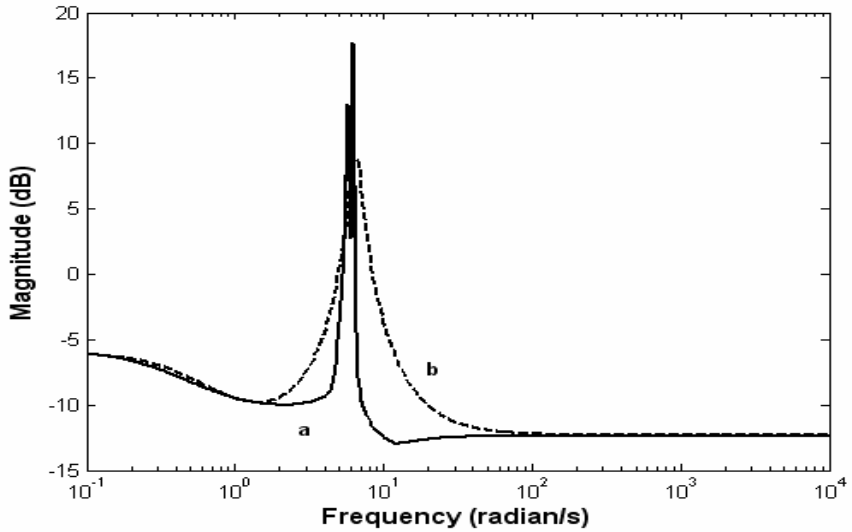

Fig. 6 (a) $sup\left|\widetilde{G}(j\omega)/G_{nom}(j\omega)-1\right|$; (b) W_2

A Butterworth filter, which satisfies the properties of $W_1(s)$, is selected as,

$$W_1(s) = \frac{K_c f_c^2}{s^3 + 2s^2 f_c + 2sf_c^2 + f_c^3} \tag{16}$$

Values of K_c=0.1 and f_c=0.05 were observed to be satisfy the requirement on the open loop transfer function L. For W_1 and W_2 selected above, and for a choice of the open-loop function L as,

$$L = \frac{10(s+32.7)(s+0.74)(s+2)}{(s+0.1)(s+20)(s+33.03)(s^2+80.42s+1677.3)} \tag{17}$$

The controller transfer function obtained through the relation C=L/P is,

$$\mathrm{K} = \frac{294.98(\mathrm{s}+0.5)(\mathrm{s}+2)}{\mathrm{s}(\mathrm{s}+0.1)} \tag{18}$$

The log-magnitude plot relating W_1, W_2 for the upper and lower bounds of L given in (12) and (13) are shown in Fig.7. The robust and nominal performance measures for the robust designs are shown in Fig.8. It can be observed that the nominal performance measure is very small relative to 0 db. The robust stability measure is marginally violated at the corner frequency. This is for a worst-case design in the absence of damping term in the electromechanical swing equation.

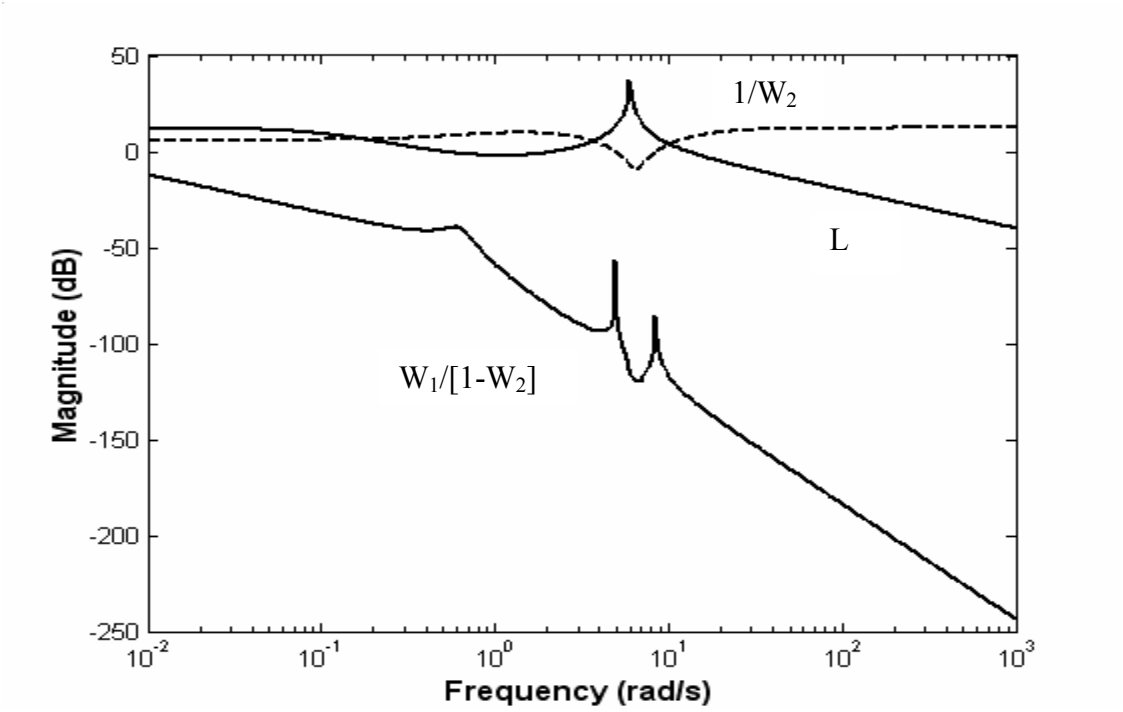

Fig. 7 The loop-shaping boundary plots

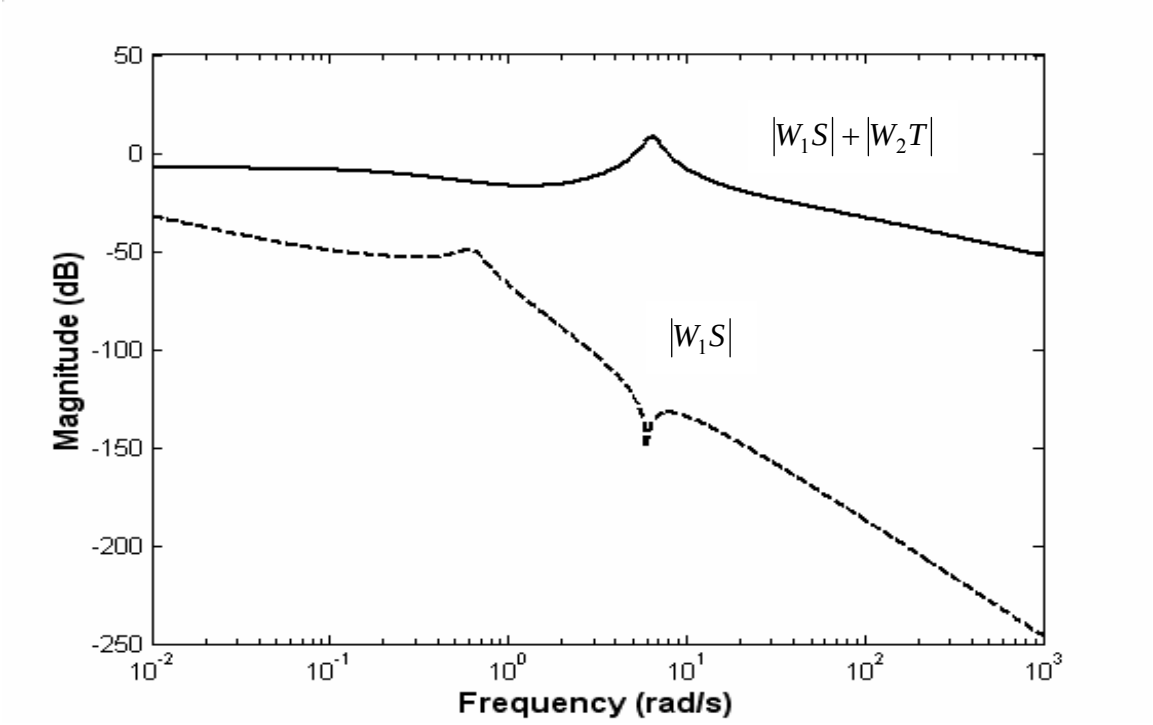

Fig. 8 Plot of nominal and robust performance indices

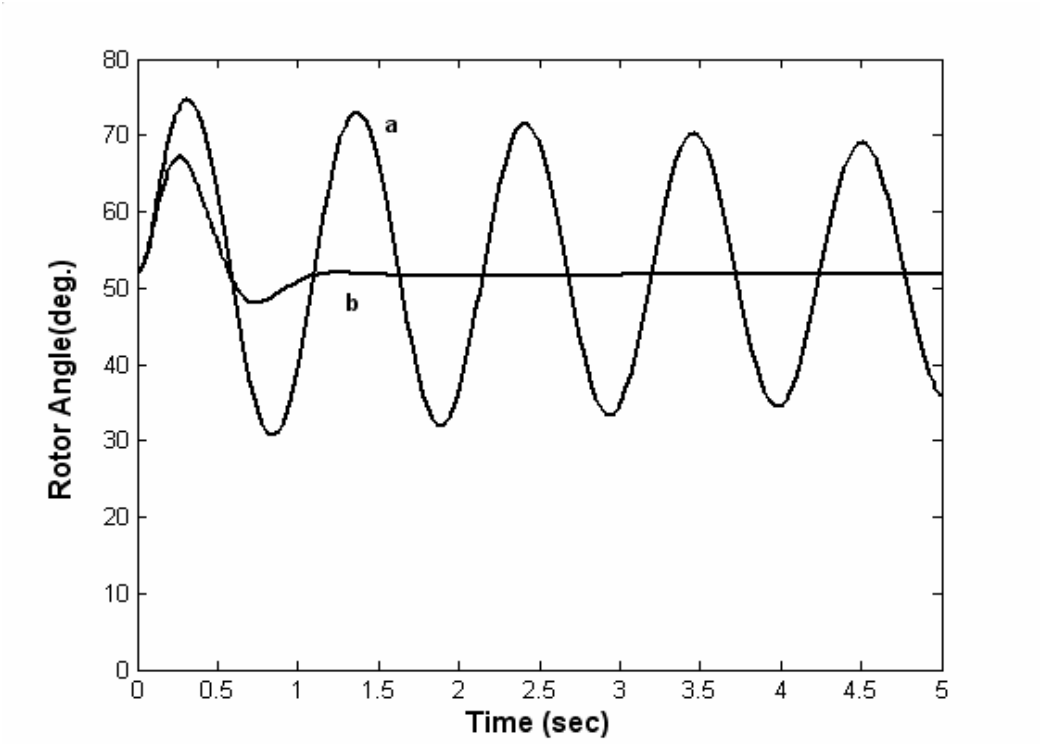

Fig.9 Generator rotor angle variation following a 50% input torque pulse for 0.1sec with, (a) no control, (b) proposed robust damping controller.

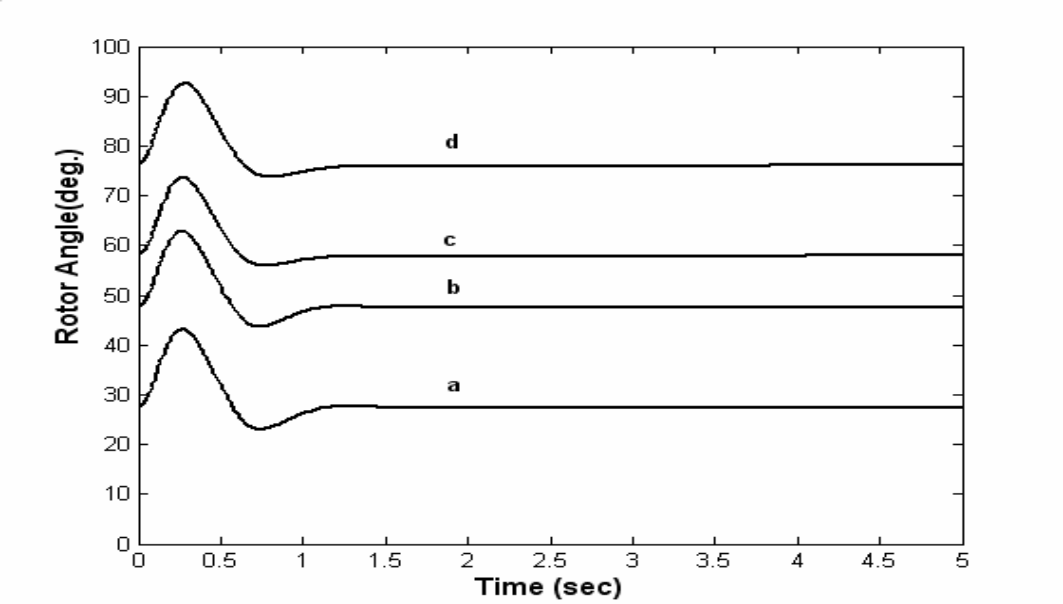

Fig.10 Rotor angle characteristics with the robust damping controller for (a) 0.5 pu output at 0.85 lagging pf, (b) 0.8 pu power at 0.9 pf lag, (c) 1pu power at 0.85 pf, and (d) 1.3 pu power at 0.95 pf lagging.

While selecting the open-loop transfer function, the internal stability of the plant in addition to the design criterion (9)-(12) had to be checked. A disturbance of 50% input torque pulse for 0.1 second on the generator shaft was simulated for this purpose. The rotor angle variations of the generator for the nominal operating point with and without the robust controller are plotted in Fig. 9. It can be observed that the no control response is extremely oscillatory; while the robust controller damps the oscillations extremely fast. The controller designed was then tested for operation on a number of other operating conditions in the range of 0.3-1.3 pu. power output. The rotor angle characteristics for 4 operating conditions are given in Fig.10 considering the same 50% torque pulse disturbance. As can be observed, the robust controller provides extremely good damping to the electromechanical oscillations for all these cases. The terminal voltage recoveries are also extremely fast as depicted in Fig. 11.

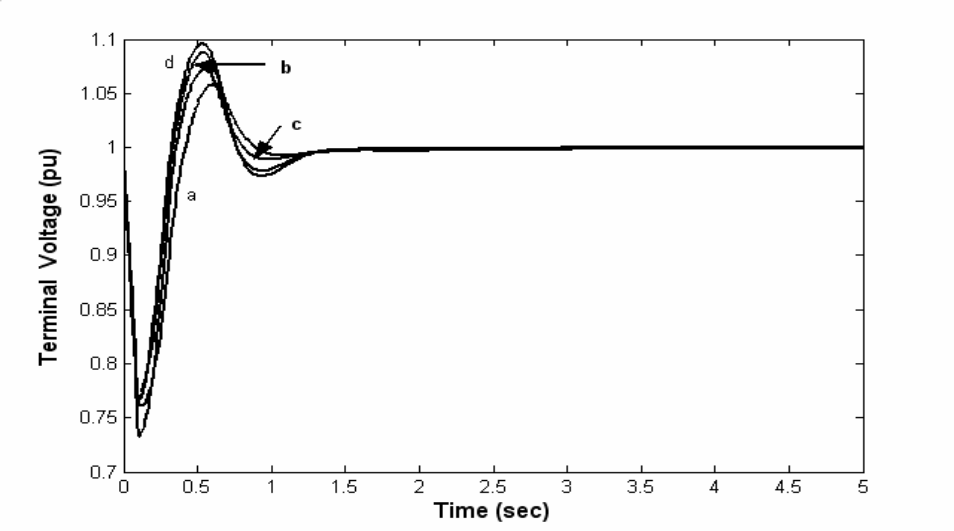

Fig. 11 Terminal voltage variations of the generator corresponding to Fig. 9

For a 3-ϕ fault of 0.05 sec on the remote bus, the rotor angle variations for the 4 operating are plotted in Fig.12. The generator terminal voltage variations and the line flows are shown in Figs 13 and 14, respectively. Without the control the response varies between very oscillatory and first swing unstable, depending on the loading conditions. As can be observed the robust controller is able to stabilize the system in a very short period for all these operating conditions. While the controller could be designed to provide even more damping, it would have to be compromised with terminal voltage transients.

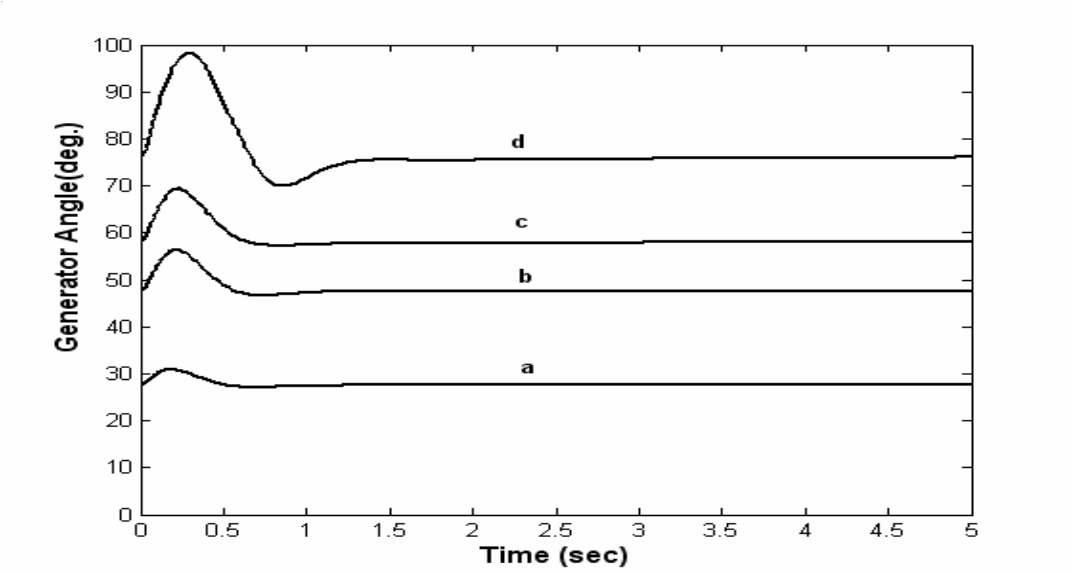

Fig. 12 Generator rotor angle variations with the robust controller following a three-phase fault for, a) 0.5 pu power output at 0.85 pf lag, b)0.8 pu at 0.9 pf lag, c)1pu at 0.85 pf lag and, d)1.3 pu at 0.95 lagging pf.

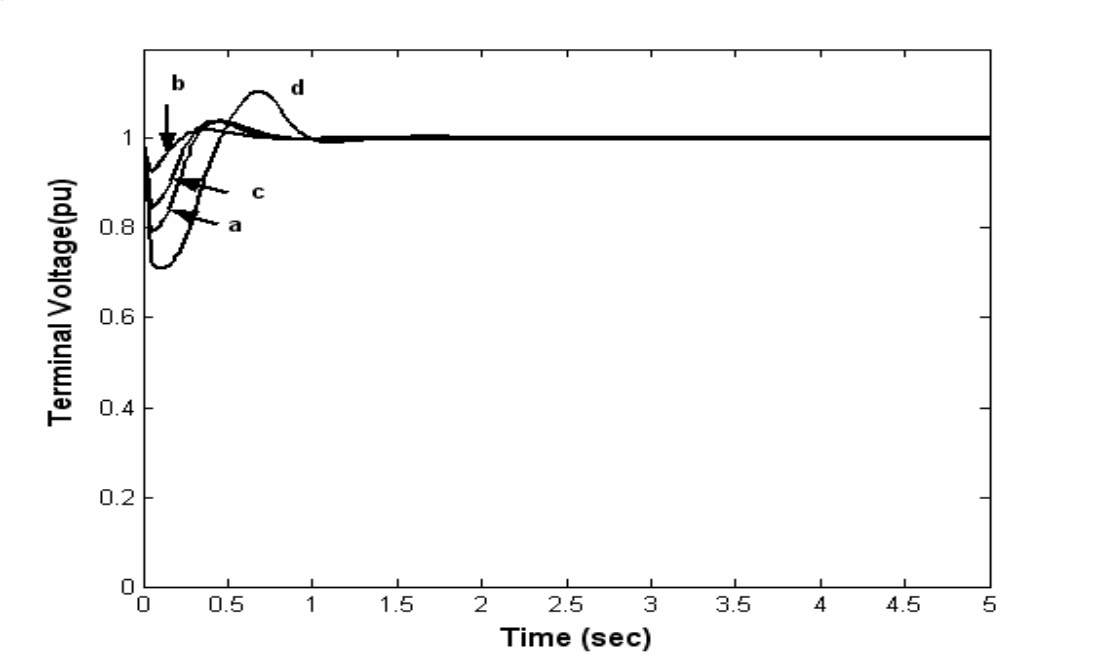

Fig. 13 Terminal voltage variations corresponding to Fig. 12

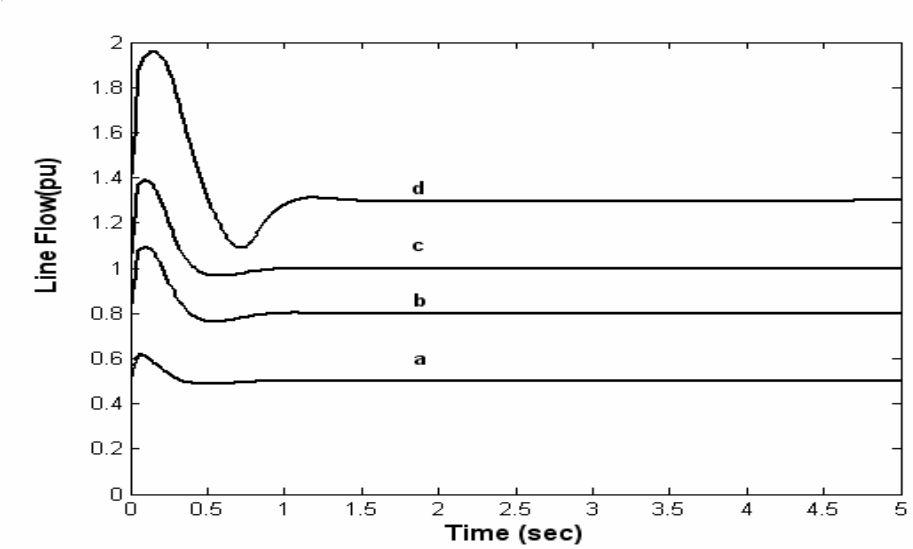

Fig. 14 The real power flow in the line with robust controller following the fault condition corresponding to Fig. 12.

5. Conclusions

A robust damping controller has been designed for a static var system employing a novel graphical method. The graphical loop-shaping technique has been employed to facilitate the design of the controller satisfying the robust stability and performance specifications in the H-∞ based design procedure. The design starts by a choice of the open-loop function, subject to a set of constraints, and ends up with a fixed parameter controller function. The controller designed was tested over a range of operating conditions with various disturbance conditions including symmetrical three-phase faults. The robust design has been found to be very effective for damping control over the range of operation designed for. The graphical loop-shaping method utilized to determine the controller function is simple and is straightforward to implement.

6. Acknowledgement

The authors wish to acknowledge the facilities provided at the K.F. University of Petroleum and Minerals. This work was performed under KFUPM sponsored research EE/ROBUST/252.

7. References

[1] A.E.Hamad, "Analysis of power system stability enhancement by static var compensators", IEEE Trans. on Power Systems, Vol. 1, no. 4, pp. 222-227, 1986.

[2] S.H.Hosseini and O.Mirshekhar, “Optimal Control of SVC for Subsynchrnous Resonance Stability in Typical Power System”, Proc. ISIE, Vol.2, pp.916-921, 2001.

[3] P.L.So and T. Yu, “Coordination of TCSC and SVC for Inter area Stability Enhancement”, Proc. POWERCON 2000, Vol.1, pp.553-558, 2000.

[4] S.E.M. Oliveria, "Synchronizing and damping torque coefficients and power system steady state stability as affected by static var compensators", IEEE Trans. on Power Systems, Vol.9, no. 1, pp.109 - 116, 1994.

[5] E.Z.Zhou, "Application of static var compensators to increase power system damping", IEEE Trans. on Power Systems, Vol. 8, no. 2. pp. 655- 661, 1993.

[6] Q. Zhao and J. Jiang, "Robust SVC Controller Design for Improving Power System Damping", IEEE Trans. Power System, Vol. 10, no. 4, pp.1927-1932, Nov. 1995.

[7] S.K.Tso, J. Liang, Q.Y. Zeng, K.L.Lo and X.X. Zhow, "Coordination of TCSC and SVC for Stability Improvement of Power Systems", Proc. 4th Intl. Conf. on Advances in power System Control, Operation and Management, APSCOM-97, Hong Kong, pp.371-376, Nov. 1997.

[8] Y. Wang, Y. Tan and G. Guo, "Robust Non-linear Coordinated Excitation and SVC Control for Power Systems", Proc. 4th APSCOM-97, Hong Kong, pp.415-420, Nov. 1997.

[9] C.Zhang and X.X. Zhou, "Coordinated Non-linear Control of TCSC and SVC in Power Systems", Proc. POWERCON '98, Vol. 1, pp.338-343, Aug. 98.

[10] R.Ghazi, A.Azemi, and K.P.Badakhushan, "Adaptive Fuzzy Sliding Mode Control of SVC and TCSC for Improving the Dynamic Performance of a Power System", Proc. 7th Intl. Conf. on AC-DC Power Transmission, pp.333-337, 2001.

[11] A.H.M.A.Rahim and S.G.A.Nassimi, "Synchronous Generator Damping Enhancement through Coordinated Control of Exciter and SVC", IEE Proc-Gener. Transm. Ditrib., Vol. 143, no. 2, pp. 221-218, March 1996.

[12] M.M.Farasangi, Y.H.Song and Y.Z.Sun, "Supplementary Control Design of SVC and STATCOM Using H_∞ Optimal Robust Control", Proc.Int. Conf. on Electric Utility Deregulation 2000, City University London, April 2000, pp. 355-360.

[13] Q. Zhao and J. Jiang, "Robust SVC Controller Design for Improving Power System damping", IEEE Trans. Power System, Vol. 10, no. 4, pp.1927-1932, Nov. 1995.

[14] J.C.Doyle, B.A. Francis, A.R.Tannenbaum, "Feedback Control Theory", MacMillan Publishing Co, New York, 1992.

[15]A.H.M.A.Rahim and S.A.Al-Baiyat, "A Robust Design of a Static VAR Compensator Controller for Power System Stability Improvement", Summer Computer Simulation Conference (SCSC'03), Article # S055, Montreal, Canada, July 2003.

[16] A. Chao and M. Athans, "Stability robustness to unstructured uncertainty for linear time invariant systems", *The Control Handbook (Editor, W.S. Levine)*, CRC Press and IEEE Press, 1996.

Appendix

The system data in pu (except stated otherwise) are [11]

R = 0.01	X = 0.3	g =0.04	b = -.38	x_d' =0.45	K_s =20
x_d =1.7	x_q =1.25	H= 4 sec	K_A = 4.0	T_A =0.03 sec	T_s=0.05

The nominal operating quantities are

v_t =1.0 P=0.866 Q= 0.392 v_o = 1.0 $\delta = 52^0$ e_q' =1.1808